Inorg. Chem. **2007**, *46*, 6529–6534

Substituent Effects on the Structures of Silver Complexes with Monoazatrithia-12-Crown-4 Ethers Bearing Substituted Aromatic Rings

Yoichi Habata,*,†,‡ Kanae Noto,† and Futoshi Osaka†

Department of Chemistry, Faculty of Science, Toho University, Funabashi, Chiba 274-8510, Japan, and Research Center for Materials with Integrated Properties, Toho University, 2-2-1 Miyama, Funabashi, Chiba 274-8510, Japan

Received March 21, 2007

New 4′-methoxybenzyl-, 4′-methylbenzyl-, benzyl-, 3′,5′-difluorobenzyl-, 3′,5′-dichlorobenzyl-, and 4′-nitrobenzyl-armed monoazatrithia-12-crown-4 ethers were prepared by the reductive amination of monoazatrithia-12-crown-4 with the appropriate benzenecarbaldehyde in the presence of $NaBH(OAc)_3$. Cold electrospray ionization mass spectrometry and X-ray crystallography show that silver complexes with armed monoazatrithia-12-crown-4 ethers bearing aromatic side arms with electron-donating groups or electron-withdrawing groups are coordination polymers and trimers, respectively. The structures of the silver complexes were strongly dependent on the strength of the CH···π interactions, which are controlled by substituent effects on the aromatic side arms.

Introduction

Many kinds of sulfur-containing macrocyclic ligands such as thia-,[1a] oxathia-,[1b] and azathiacrown ethers[1c] have been prepared in order to develop new ligands with specific binding properties for transition-metal ions. During our research efforts on the development of new armed azacrown and azathiacrown ethers, we reported that a diazahexathia-24-crown-8 ether bearing the 3′,5′-dichlorobenzyl group as side arms incorporated two Ag^+ ions in the crown ring, and the aromatic side arms enclosed the Ag^+ ions.[2] On the other hand, two phenylethyl-appended diazahexathia-24-crown-8 ethers formed a polymer, and the aromatic side arms do not participate in coordination in the solid state. These results indicate that the aromatic side arm plays a key part in the binding of Ag^+ ions and substituent effects of the aromatic side arms may affect the structures of the silver complexes.

Recently, increasing attention has been focused on the significance of CH···π interaction in supramolecular structures and organic reactions.[3] Although the CH···π interaction is a weak interaction, significant effects on the overall structure are possible when the interaction occurs in polymeric systems. Here we report that the structures of silver complexes with the aromatic armed monoazatrithia-12-crown-4 (**2a**−**2f**) are changed drastically by CH···π interactions, which are controlled by the substituent effect on the aromatic side arms.

Experimental Section

Melting points were obtained with a Mel-Temp capillary apparatus and were not corrected. Fast atom bombardment mass spectrometry (FAB-MS) spectra were obtained using a JEOL 600 H mass spectrometer. ^{1}H NMR spectra were measured in $CDCl_3$ on a JEOL ECP400 (400 MHz) spectrometer. Cold electrospray ionization mass spectrometry (ESI-MS) spectra were recorded on

* To whom correspondence should be addressed. E-mail: habata@chem.sci.toho-u.ac.jp.

† Department of Chemistry, Faculty of Science.

‡ Research Center for Materials with Integrated Properties.

(1) (a) Katritzky, A. R., Rees, C. W., Scriven, E. F. V., Eds. *Comprehensive Heterocyclic Chemistry II*; Elsevier: Oxford, U.K., 1995; Vol. 9, Chapter 30. Edema, J. J. H.; Buter, J.; Kellogg, R. M. *Tetrahedron* **1994**, *50*, 2095. Blake, A. J.; Li, W.; Lippolis, V.; Schröder, M. *Chem. Commun*. **1997**, 1943. Blake, A. J.; Devillanova, F. A.; Garau, A.; Gilvy, L. M.; Gould, R. O.; Isaia, F.; Lippolis, V.; Parsons, S.; Radek, C.; Schröder, M. *J. Chem. Soc., Dalton Trans*. **1998**, 2037. Blake, A. J.; Li, W.; Lippolis, V.; Taylor, A.; Schröder, M. *J. Chem. Soc., Dalton Trans*. **1998**, 2931. Blake, A. J.; Fenske, D.; Li, W.; Lippolis, V.; Schröder, M. *J. Chem. Soc., Dalton Trans*. **1998**, 3961. Blake, A. J.; Devillanova, F. A.; Garau, A.; Isaia, F.; Lippolis, V.; Parsons, S.; Schroder, M. *J. Chem. Soc., Dalton Trans*. **1999**, 525. (b) Katritzky, A. R., Rees, C. W., Scriven, E. F. V., Eds. *Comprehensive Heterocyclic Chemistry II*; Elsevier: Oxford, U.K., 1995; Vol. 9, Chapter 32. (c) van de Water, L. G. A.; Hoonte, F.; Driessen, W. L.; Reedijk, J.; Sherrington, D. C. *Inorg. Chim. Acta* **2000**, *303*, 77. Tanaka, M.; Nakamura, M.; Ikeda, T.; Ikeda, K.; Ando, H.; Shibutani, Y.; Yajima, S.; Kimura, K. *J. Org. Chem*. **2001**, *66*, 7008. Love, J. B.; Vere, J. M.; Glenny, M. W.; Blake, A. J.; Schröder, M. *Chem. Commun*. **2001**, 2678. Tanaka, M.; Ikeda, T.; Xu, Q.; Ando, H.; Shibutani, Y.; Nakamura, M.; Sakamoto, H.; Yajima, S.; Kimura, K. *J. Org. Chem*. **2002**, *67*, 2223. Caltagirone, C.; Bencini, A.; Demartin, F.; Devillanova, F. A.; Garau, A.; Isaia, F.; Lippolis, V.; Mariani, P.; Papke, U.; Tei, L.; Verani, G. *Dalton Trans.* **2003**, 901.

(2) Habata, Y.; Seo, J.; Otawa, S.; Osaka, F.; Noto, K.; Lee, S. S. *Dalton Trans.* **2006**, 2202.

(3) (a) Nishio, M. *CrystEngComm* **2004**, *6*, 130. (b) Nishio, M. *Tetrahedron* **2005**, *61*, 6923.

10.1021/ic700538f CCC: $37.00
Published on Web 07/13/2007

Table 1. Crystal Data and Refinement Parameters for Complexes **2a**−$AgPF_6$, **2b**−AgOTf, **2c**−AgOTf, **2d**−AgOTf, **2e**−AgOTf, and **2f**−AgOTf

compound	**2a**−$AgPF_6$	**2b**−AgOTf
formula	$C_{18}H_{28}N_2OS_3F_6PAg$	$C_{19}H_{28}N_2O_3S_4F_3Ag$
M	637.44	625.54
T/K	90	298
cryst syst	orthorhombic	monoclinic
space group	$P2(1)2(1)2(1)$	$P2(1)/c$
a/Å	8.7234(6)	13.8910(8)
b/Å	14.5024(11)	9.0832(5)
c/Å	20.6747(16)	23.7127(10)
α/deg		
β/deg		122.378(2)
γ/deg		
U/Å^3	2615.6(3)	2526.8(2)
Z	4	4
D_c/g cm^{-3}	1.619	1.644
μ/mm^{-1}	1.127	1.174
reflns collecd	19 031	18 228
unique reflns, R_{int}	3655, 0.0398	6255, 0.0555
R_F[a]	0.0332 [3450, $I > 2\sigma(I)$]	0.0438 [4173, $I > 2\sigma(I)$]
R_F, $Rw(F^2)$ (all data)[a]	0.0361, 0.0896	0.0688, 0.0947
compound	**2c**−AgOTf	**2d**−AgOTf
formula	$C_{36}H_{52}N_4O_6S_8F_6Ag_2$	$C_{19}H_{27}NO_4S_4F_5Ag$
M	1223.04	664.53
T/K	298	90
cryst syst	monoclinic	orthorhombic
space group	$P2(1)/c$	$P2(1)2(1)2(1)$
a/Å	24.854(2)	9.5868(6)
b/Å	8.9828(9)	11.6802(7)
c/Å	23.438(2)	22.3982(14)
α/deg		
β/deg	109.941(2)	
γ/deg	78.20(2)	
U/Å^3		2508.1(3)
Z	4	4
D_c/g cm^{-3}	1.651	1.760
μ/mm^{-1}	1.204	1.201
reflns collecd	13 360	18 807
unique reflns, R_{int}	8998, 0.0359	3532, 0.0311
R_F[a]	0.0442 [4775, $I > 2\sigma(I)$]	0.0312 [3421, $I > 2\sigma(I)$]
R_F, $Rw(F^2)$ (all data)[a]	0.0915, 0.0966	0.0322, 0.0744
compound	**2e**−AgOTf	**2f**−AgOTf
formula	$C_{50}H_{73}N_3O_{12}S_{12}Cl_6F_9Ag_3$	$C_{56}H_{72}N_{10}O_{15}S_{12}F_9Ag_3$
M	2000.14	2004.57
T/K	100	298
cryst syst	triclinic	trigonal
space group	$P\bar{1}$	$R\bar{3}$
a/Å	8.7183(4)	20.7184(7)
b/Å	21.1087(10)	20.7184(7)
c/Å	22.2440(10)	32.921(2)
α/deg	72.1060(10)	
β/deg	82.9840(10)	
γ/deg	83.0890(10)	120
U/Å^3	3851.5(3)	12238.2(11)
Z	2	6
D_c/g cm^{-3}	1.725	1.632
μ/mm^{-1}	1.364	1.103
reflns collecd	29003	28775
unique reflns, R_{int}	18920, 0.0271	6238, 0.0479
R_F[a]	0.0567 [14 771, $I > 2\sigma(I)$]	0.0758 [4515, $I > 2\sigma(I)$]
R_F, $Rw(F^2)$ (all data)[a]	0.0752, 0.1619	0.0949, 0.2461

[a] $R_F = \sum||F_o| - |F_c||/\sum|F_o|$. $Rw(F^2) = [\sum w|F_o^2 - F_c^2|^2/\sum wF_o^4)]^{1/2}$.

a JEOL JMS-T100CS mass spectrometer. 1,4,7-Trithia-10-azacyclododecane (monoazatrithia-12-crown-4, **1**) was prepared as previously reported.[2]

Preparation of Armed Monoazatrithia-12-crown-4 Ethers. *N*-(4′-Methoxybenzyl)-1,4,7-trithia-10-azacyclododecane (2a). After a mixture of 4-methoxybenzaldehyde (2.0 mmol) and **1** (1.0 mmol) in dry 1,2-dichloroethane (25 mL) was stirred at room temperature for 1 day under an argon atmosphere (1 MPa), triacetoxysodium borohydride (2.0 mmol) was added, and the mixture was stirred for a further 1 day at room temperature. Saturated aqueous Na_2CO_3 was added, and the aqueous layer was extracted with chloroform (20 mL × 3). The combined organic layer was washed with water, dried over Na_2SO_4, and concentrated. The residual oil was recrystallized from hexane to give **2a** in 40% yield.

Mp: 124−125 °C. ^{1}H NMR ($CDCl_3$): δ 7.24 (d, J = 8.8 Hz, 2H), 6.85 (d, J = 8.8 Hz, 2H), 3.78 (s, 3H), 3.57 (s, 2H), 2.79 (s, 8H), 2.73 (t, J = 7.73 Hz, 4H), 2.63 (t, J = 7.73 Hz, 4H). FAB-MS (matrix: *m*-NBA): *m/z* 344 ([M + 1]$^+$, 100%). Anal. Calcd for $C_{16}H_{25}NOS_3$: C, 55.93; H, 7.33; N, 4.08. Found: C, 55.51; H, 7.18; N, 3.96.

***N*-(4′-Methylbenzyl)-1,4,7-trithia-10-azacyclododecane (2b).** The preparation procedure was the same as that used for **2a**. Yield: 43%. Mp: 85.0−86.0 °C. ^{1}H NMR ($CDCl_3$): δ 7.20 (d, J = 7.78 Hz, 2H), 7.12 (d, J = 7.78 Hz, 2H), 3.61 (s, 2H), 2.74−2.81 (m, 12H), 2.63 (t, J = 7.21 Hz, 4H), 2.34 (s, 3H). FAB-MS (matrix: *m*-NBA): *m/z* 328 ([M + 1]$^+$, 20%). Anal. Calcd for $C_{16}H_{25}NS_3$: C, 58.66; H, 7.69; N, 4.28. Found: C, 58.49; H, 7.67; N, 3.88.

***N*-Benzyl-1,4,7-trithia-10-azacyclododecane (2c).** The preparation procedure was the same as that used for **2a**. Yield: 21%. Mp: 106−107 °C. ^{1}H NMR (CD_2Cl_2): δ 7.20−7.29 (m, 5H), 3.65 (s, 2H), 2.82 (s, 8H), 2.78 (t, J = 7.6 Hz, 4H), 2.64 (t, J = 7.6 Hz, 4H). FAB-MS (matrix: 1:1 DTT/TG): *m/z* 314 ([M + 1]$^+$, 100%). Anal. Calcd for $C_{15}H_{23}NS_3$: C, 57.46; H, 7.39; N, 4.47. Found: C, 57.42; H, 7.34; N, 4.16.

***N*-(3′,5′-Difluorobenzyl)-1,4,7-trithia-10-azacyclododecane (2d).** The preparation procedure was the same as that used for **2a**. Yield: 20%. Mp: 88.5−89.3 °C. ^{1}H NMR (CD_2Cl_2): δ 6.94 (dd, J_1 = 2.0 Hz, J_2 = 8.4 Hz, 2H), 6.71 (tt, J_1 = 2.8 Hz, J_2 = 8.7 Hz, 1H), 3.62 (s, 2H), 2.67 (t, J = 6.4 Hz, 4H). FAB-MS (matrix: *m*-NBA): *m/z* 350 ([M + 1]$^+$, 100%). Anal. Calcd for $C_{15}H_{21}F_2NS_3 \cdot {}^1/_4H_2O$: C, 50.89; H, 6.12; N, 3.96. Found: C, 50.78; H, 6.34.

***N*-(3′,5′-Dichlorobenzyl)-1,4,7-trithia-10-azacyclododecane (2e).** The preparation procedure was the same as that used for **2a**. Yield: 29%. Mp: 115.0−115.5 °C. ^{1}H NMR (CD_2Cl_2): δ 7.302 (s, 2H), 7.268 (s, 1H), 3.587 (s, 2H), 2.813 (s, 8H), 2.746 (t, J = 6.78 Hz, 4H), 2.645 (t, J = 7.18 Hz, 4H). FAB-MS (matrix: *m*-NBA): *m/z* 383 ([M + 1]$^+$, 84%). Anal. Calcd for $C_{15}H_{21}Cl_2NS_3$: C, 47.11; H, 5.53; N, 3.66. Found: C, 47.07; H, 5.50; N, 3.56.

***N*-(4′-Nitrobenzyl)-1,4,7-trithia-10-azacyclododecane (2f).** The preparation procedure was the same as that used for **2a**. Yield: 40%. Mp: 126−128 °C. ^{1}H NMR (CD_2Cl_2): δ 8.20 (d, J = 8.8 Hz, 2H), 7.55 (d, J = 8.8 Hz, 2H), 3.73 (s, 2H), 2.84 (s, 8H), 2.77 (t, J = 4.8 Hz, 4H), 2.64 (t, J = 4.8 Hz, 4H). FAB-MS (matrix: *m*-NBA): *m/z* 359 ([M + 1]$^+$, 30%). Anal. Calcd for $C_{15}H_{22}N_2O_2S_3$: C, 50.25; H, 6.18; N, 7.81. Found: C, 50.15; H, 6.14; N, 7.91.

Preparation of Silver Complexes. AgOTf or $AgPF_6$ (0.03 mmol) in methanol (1 mL) was treated with the **2** host (0.01 mmol) in acetonitrile (1 mL). Crystals of the corresponding silver complex were obtained quantitatively upon evaporation of the solvent.

2a−**$AgPF_6$.** Mp: >160 °C (dec). Anal. Calcd for $C_{16}H_{25}NOS_3$-$AgPF_6 \cdot CH_3OH$: C, 32.49; H, 4.65; N, 2.23. Found: C, 32.81; H, 4.20; N, 2.06.

Table 2. Normalized Cold ESI-MS Intensities of Fragment Ion Peaks of Silver Complexes (L = Ligand, S = Solvent, and A = Anion)

	2a + AgOTf	**2a** + $AgPF_6$	**2b** + AgOTf	**2c** + AgOTf	**2d** + AgOTf	**2e** + AgOTf	**2f** + AgOTf
substituents	CH_3O	CH_3O	CH_3	H	F	Cl	NO_2
$[L + Ag]^+$	100.0	100.0	100.0	100.0	100.0	100.0	100.0
$[2L + 2Ag + S]^+$	16.6					3.1	7.2
$[2L + 2Ag + A]^+$	5.9	4.8	20.5	11.0	13.7	3.6	8.5
$[3L + 3Ag + A + S]^+$	0.9						
$[3L + 3Ag + 2A]^+$	1.1	0.8	6.1	1.5	2.1	0.8	0.6
$[4L + 4Ag + 2A + S]^+$	0.5						
$[4L + 4Ag + 3A]^+$	0.5	0.7	4.5	1.1	0.9		
$[4L + 5Ag + 4A]^+$		0.4					
$[4L + 6Ag + 5A]^+$		0.2					
$[5L + 5Ag + 4A]^+$			3.0	1.0	0.4		
$[5L + 6Ag + 5A]^+$		0.2					
$[6L + 6Ag + 5A]^+$			1.9	0.6			
$[7L + 7Ag + 6A]^+$			1.6	0.3			

2b−AgOTf. Mp: >185 °C (dec). Anal. Calcd for $C_{17}H_{25}NO_3S_4F_3Ag\cdot{}^1/_2CH_3CN$: C, 35.73; H, 4.41; N, 3.47. Found: C, 35.63; H, 4.52; N, 3.49.

2c−AgOTf. Mp: >177 °C (dec). Anal. Calcd for $C_{16}H_{23}NO_3S_4F_3Ag\cdot{}^3/_4H_2O$: C, 33.69; H, 4.06; N, 2.46. Found: C, 32.91; H, 4.23; N, 2.40.

2d−AgOTf. Mp: >165 °C (dec). Anal. Calcd for $C_{16}H_{21}NO_3S_4Ag\cdot CH_3CN$: C, 33.39; H, 3.74; N, 4.33. Found: C, 33.30; H, 3.81; N, 3.95. Single crystals for X-ray analysis were obtained by further recrystallization from acetone.

2e−AgOTf. Mp: >120 °C (dec). Anal. Calcd for $C_{16}H_{21}NO_3S_4Cl_2F_3Ag\cdot{}^1/_2H_2O$: C, 29.64; H, 3.42; N, 2.16. Found: C, 29.67; H, 3.48; N, 1.76.

2f−AgOTf. Mp: >115 °C (dec). Anal. Calcd for $C_{16}H_{22}N_2O_5S_4F_3Ag\cdot CH_3OH$: C, 31.53; H, 4.05; N, 4.33. Found: C, 31.75; H, 3.72; N, 4.09.

X-ray Structure Determination. Crystals of AgOTf or $AgPF_6$ complexes with **2a**−**2e** were mounted on the tip of a glass fiber, and data collection was carried out on a Bruker SMART diffractometer equipped with a CCD area detector at 90−298 K. The data were corrected for Lorentz and polarization effects, and absorption corrections were applied with the *SADABS*[4] program. The structures were solved by direct methods and subsequent difference Fourier syntheses using the program *SHELX*.[5] All non-H atoms were refined anisotropically, and H atoms were placed in calculated positions and thereafter refined with $U_{iso}(H) = 1.2U_{eq}(C)$. The crystallographic refinement parameters of **2a**−$AgPF_6$, **2b**−AgOTf, **2c**−AgOTf, **2d**−AgOTf, **2e**−AgOTf, and **2f**−AgOTf are summarized in Table 1, while selected bond distances and angles and close CH···π distances of these complexes are listed in Tables 3 and 4, respectively.

Calculation of the Electrostatic Potential Isosurfaces. Density functional theory (DFT) calculations (B3LYP/6-31G*)[6] using 6-31G* as an initial geometry were performed using *Spartan 04*[7] computer modeling software. The isosurface values of the substituted benzene derivatives are displayed at 8.1 electrons/au.[3]

Results and Discussion

New armed monoazatrithia-12-crown-4 ethers bearing substituted aromatic ring pendants were prepared by the reaction of monoazatrithia-12-crown-4 (**1**)[2] with the appropriate substituted benzenecarbaldehyde in the presence

Table 3. Selected Bond Distances (Å) and Angles (deg)

	2a−$AgPF_6$	**2b**−AgOTf	**2c**−AgOTf
Ag1−N1	2.532(4)	2.526(2)	2.538(4)
Ag1−S1	2.6010(13)	2.6374(9)	2.5777(14)
Ag1−S2	2.7600(11)	2.7973(8)	2.8205(14)
Ag1−S3	2.6467(12)	2.6035(9)	2.6416(14)
Ag1−S2A	2.5217(11)	2.5357(8)	2.5197(13)
Ag2−N2			2.529(4)
Ag2−S4			2.6290(15)
Ag2−S5			2.8001(13)
Ag2−S6			2.5872(15)
Ag2−S5A			2.5202(13)
N1−Ag1−S2A	119.91(9)	110.62(6)	112.158(10)
N2−Ag2−S5A			112.56(11)
Ag1−S2−Ag1A	144.56(5)	146.44(3)	144.64(5)
Ag2−S5−Ag2A			145.75(5)

	2d−AgOTf	**2e**−AgOTf	**2f**−AgOTf
Ag1−N1	2.524(3)	2.485(4)	2.529(5)
Ag1−S1	2.5805(15)	2.6257(14)	2.705(2)
Ag1−S2	3.0096(10)	2.7589(13)	2.7700(16)
Ag1−S2A	2.5280(10)		2.4882(16)
Ag1−S3	2.5554(10)	2.5997(14)	2.5616(18)
Ag1−S8		2.4767(13)	
Ag2−N2		2.553(4)	
Ag2−S4		2.6065(14)	
Ag2−S5		2.8501(13)	
Ag2−S6		2.6033(14)	
Ag2−S2		2.5121(12)	
Ag3−N3		2.576(4)	
Ag3−S7		2.6446(15)	
Ag3−S8		2.8609(13)	
Ag3−S9		2.5814(14)	
Ag3−S5		2.5288(12)	
N1−Ag1−S2A	106.76(8)		121.70(12)
N1−Ag1−S8		120.78(10)	
N2−Ag2−S2		126.13(10)	
N3−Ag3−S5		131.39(10)	
Ag1−S2−Ag1A	147.39(4)		127.60(7)
Ag1−S2−Ag2		128.29(5)	
Ag2−S5−Ag3		131.29(5)	
Ag1−S8−Ag3		130.42(5)	

Table 4. Close CH···Benzene Plane Distances (Å)

	2a−$AgPF_6$	**2b**−AgOTf	**2c**−AgOTf	**2d**−AgOTf
H3A···benzene plane	2.999		3.194	
H4B···benzene plane		2.812		
H5A···benzene plane	2.692			2.823
H6A···benzene plane				3.444
H6B···benzene plane		3.147		3.385
H21B···benzene plane			3.187	
average	2.846	2.999	3.190	3.217

(4) Sheldrick, G. M. *SADABS, Program for absorption correction of area detector frames*; Bruker AXS, Inc.: Madison, WI, 1996.
(5) *SHELXTL*, version 5.1; Bruker AXS, Inc.: Madison, WI, 1997.
(6) Stephens, P. J.; Devlin, F. J.; Chabalowski, C. F.; Frisch, M. J. *J. Phys. Chem.* **1994**, *98*, 11623. Rauhut, G.; Pulay, P. *J. Am. Chem. Soc.* **1995**, *117*, 4167. Rauhut, G.; Pulay, P. J. *J. Phys. Chem.* **1995**, *99*, 3093.
(7) *Spartan 04*; Wavefunction, Inc.: Irvine, CA, 2003.

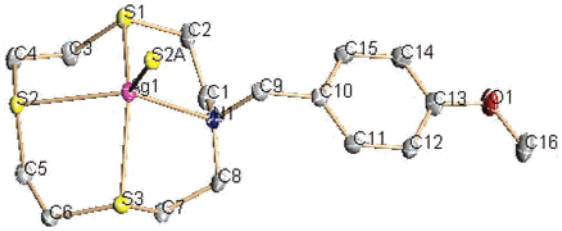

Figure 1. ORTEP diagram of **2a**−$AgPF_6$ showing thermal ellipsoids at 50% probability. H atoms, the PF_6 anion, and solvents are omitted.

of $NaBH(OAc)_3$ in 1,2-dichloroethane under 1 MPa (argon atmosphere).

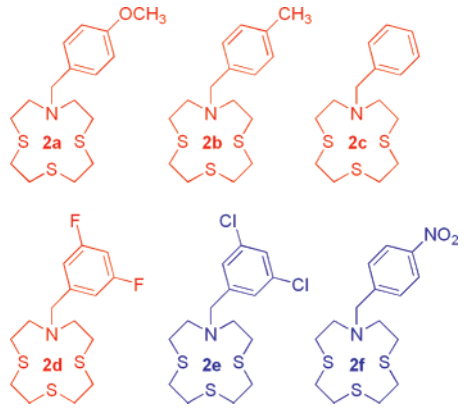

The new ligands were treated with equimolar amounts of AgOTf or $AgPF_6$ in CH_3CN, CH_3OH, or acetone to give silver triflate or silver hexafluorophosphate complexes in quantitative yields.

We have reported that cold ESI-MS is a powerful tool in the determination of structures of silver triflate complexes with pyridylmethyl-armed monoaza-12-crown-4 ethers.[8a] In keeping with this, the structures of the silver complexes with **2a**−**2f** in solution were examined by cold ESI-MS at 278 K. Intensities of normalized fragment ion peaks of the silver complexes with **2a**−**2f** are summarized in Table 2. In the cold ESI-MS of the **2a**−AgOTf and **2a**−$AgPF_6$ complexes, $[4\mathbf{2a} + 4Ag + 3OTf]^+$ and $[5\mathbf{2a} + 6Ag + 5PF_6]^+$ were observed, respectively. Higher fragment ion peaks, $[6(\mathbf{2b}$ or $\mathbf{2c}) + 6Ag + 5OTf]^+$ and $[7(\mathbf{2b}$ or $\mathbf{2c}) + 7Ag + 6OTf]^+$, were observed in the **2b**−AgOTf and **2c**−AgOTf complexes. In addition, **2d**−AgOTf, which has two F atoms on the aromatic ring, gave $[5\mathbf{2d} + 5Ag + 4OTf]^+$. Therefore, the cold ESI-MS data suggested that **2a**−**2d** would be more likely to form coordination polymers compared to a tetramer. On the other hand, **2e**−AgOTf and **2f**−AgOTf complexes showed only $[3(\mathbf{2e}$ or $\mathbf{2f}) + 3Ag + 2A]^+$ as the highest fragment ion peaks. The results show that **2e** and **2f** would form, at maximum, a trimer.

Ligands **2a**−**2e** were treated with equimolar amounts of AgOTf or $AgPF_6$ in appropriate solvents to give silver triflate or silver hexafluorophosphate complexes in quantitative yields. The structures of **2a**−$AgPF_6$, **2b**−AgOTf, **2c**−AgOTf, **2d**−AgOTf, **2e**−AgOTf, and **2f**−AgOTf complexes were determined by X-ray crystallography. Figure 1 shows

(8) (a) Habata, Y.; Yamada, S.; Osaka, F. *Inorg. Chem.* **2006**, *45*, 987. (b) Habata, Y.; Osaka, F. *Dalton Trans.* **2006**, 1836.

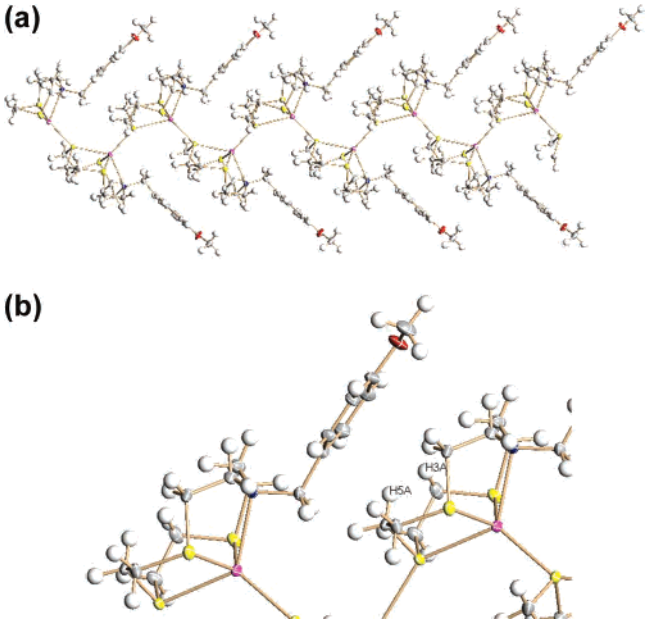

Figure 2. (a) Packing diagram of **2a**−$AgPF_6$ and (b) a partial magnified view. The PF_6 anion and solvents are omitted. A schematic drawing of the zigzag polymer structure is shown in Figure 5.

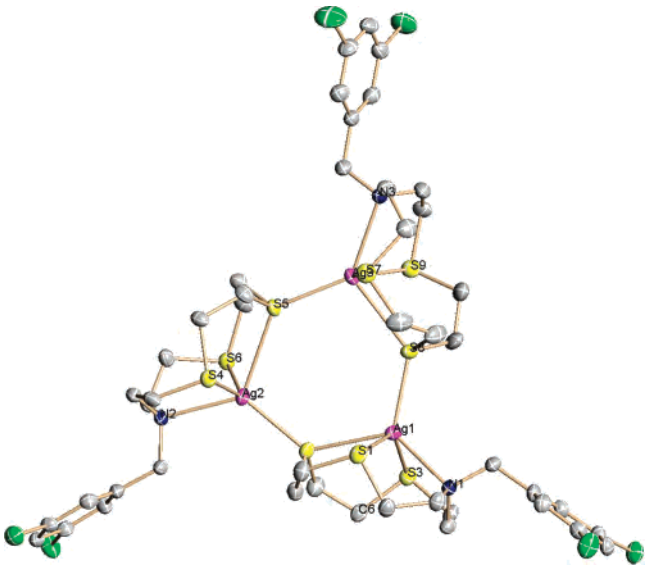

Figure 3. ORTEP diagram of the **2e**−AgOTf complex with thermal ellipsoids at 50% probability. H atoms, OTf anions, and solvents are omitted. A schematic drawing of the cyclic trimer is shown in Figure 5.

the ORTEP diagram of the **2a**−$AgPF_6$ complex. In this complex, the Ag^+ ion is five-coordinated by the ring N1, the ring S1, S2, and S3 atoms, and the S2A atom of the nearest-neighbor molecule. The Ag1−N1, Ag1−S1, Ag1−S2, Ag1−S3, and Ag1−S2A distances are 2.532, 2.601, 2.760, 2.6467, and 2.5217 Å, respectively. Selected bond distances (Å) and angles (deg) are summarized in Table 3. As shown in the packing diagram (Figure 2a), **2a**−$AgPF_6$ forms a zigzag coordination polymer. Average distances between the H atoms (H3A and H5A) of the crown ring and the benzene plane of the nearest-neighbor molecule are about 2.85 Å (Figure 2b). It is well-known that the average

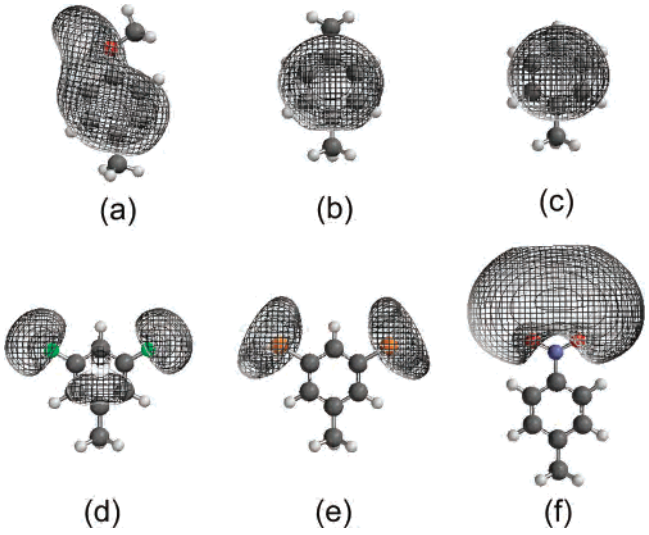

Figure 4. Electrostatic potential isosurfaces (at 8.1 electrons/au^3) of (a) 4-methoxytoluene, (b) *p*-xylene, (c) toluene, (d) 3,5-difluorotoluene, (e) 3,5-dichlorotoluene, and (f) 4-nitrotoluene.

nonbonding CH$\cdots\pi$ distance is estimated to be 2.91 Å.[3a,9] Therefore, the CH$\cdots$benzene plane distances in the **2a**−$AgPF_6$ complex are indicative of a CH$\cdots\pi$ interaction. The silver complexes with **2b**−**2d** are isomorphous. The CH$\cdots$ benzene plane distances of the other silver complexes are summarized in Table 2.

On the other hand, **2e**−AgOTf (Figure 3) and **2f**−AgOTf complexes form a cyclic trimer, in which three azatrithiacrown rings are bridged by the S2, S5, and S8 atoms at position 7 of the crown rings. In these complexes, the Ag^+ ion is five-coordinated by the ring N, three ring S atoms, and an S atom of the nearest-neighbor molecule. The average Ag−N, Ag−ring S, and Ag-bridged−S distances are 2.54, 2.67, and 2.51 Å, respectively. Kuppers et al. reported that a silver complex with trithia-9-crown-3 gives 2:1 and 3:3 (host−Ag^+) complexes in a unit cell.[10] The Ag−S distances in the **2e**−AgOTf and **2f**−AgOTf complexes are comparable with those of the 3:3 complex.

In this system, the results of the X-ray data are consistent with the cold ESI-MS data, which reflect the structures in solution.

The drastic structural change between the silver complexes with **2a**−**2d** and those with **2e** and **2f** is explained by the substituent effect on the aromatic rings. To examine the

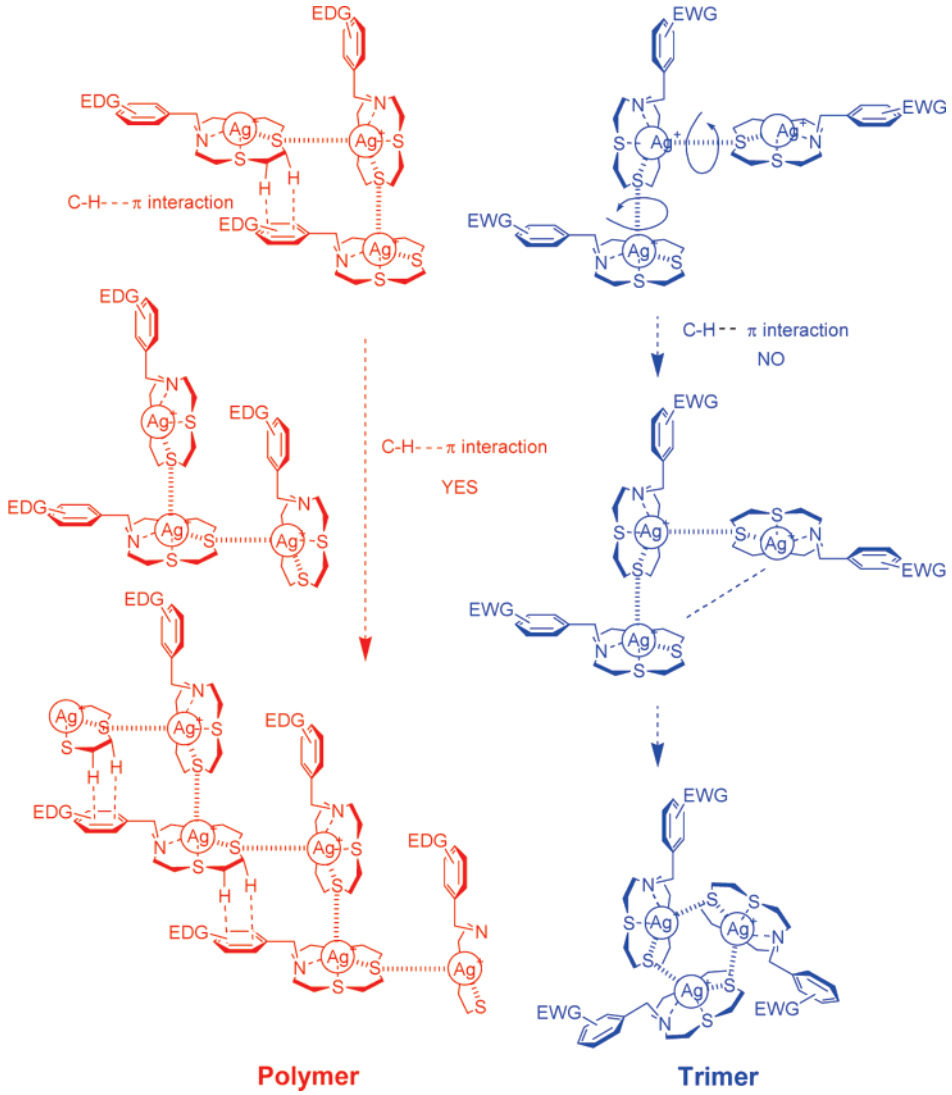

Figure 5. Postulated formation mechanism for coordination polymers and trimers. EDG = electron-donating group; EWG = electron-withdrawing group.

electron density on the aromatic side arms, we calculated electrostatic potentials for model compounds. The electrostatic potential is a function describing the energy of interaction of a point positive charge with the nuclei and the fixed charge distribution of a molecule.[11] The electrostatic potential isosurface shows the electron-rich region of the molecule. Figure 4 shows the electrostatic potential isosurfaces (at 8.1 electrons/au^3) of substituted toluenes that were calculated by the DFT (B3LYP/6-31G*) method. As shown in Figure 4, 4-methoxytoluene, *p*-xylene, toluene, and 3,5-difluorotoluene have electron-rich regions among the C atoms on the aromatic rings, while 3,5-dichlorotoluene and 4-nitrotoluene do not have electron-rich regions on the aromatic rings. Interestingly, the average CH···benzene plane distances of the silver complexes with **2a**−**2e** (Table 4) are lengthened with a decrease in the electron density on the aromatic rings (the CH···benzene plane distance: **2a** < **2b** < **2c** < **2d**). Suezawa et al. reported an electronic substituent effect on intramolecular CH···π interaction in 4-substituted aromatic compounds by nuclear overhauser enhancement (NOE) experiments.[12] The order of the CH···benzene plane distances in the silver complexes with **2a**, **2b**, **2c**, and **2f** that have 4′-substituted aromatic rings is exactly the same as that of the NOE experiments. These results clearly suggest that the strength of the CH···π interaction depends on the electron density on the aromatic rings.

The cold ESI-MS, X-ray crystallography, and calculation of the electrostatic potential isosurfaces lead us to describe a formation mechanism for the coordination polymers and trimers (Figure 5). When the electron density on the aromatic side arm is relatively high, the CH···π interaction may act so as to encourage the formation of the polymeric structures. On the other hand, when the electron density on the aromatic ring is low, the interaction is nonexistent, and the trimers form.

In conclusion, we have demonstrated that the silver complexes with compounds **2a**−**2d** bearing aromatic side arms with electron-donating groups and compounds **2e** and **2f** having aromatic side arms with electron-withdrawing groups form coordination polymers and trimers, respectively. These results indicate that the structures of silver complexes with monoazatrithia-12-crown-4 bearing substituted aromatic rings can be changed drastically by the strength of the CH···π interactions, which are controlled by substituent effects on the aromatic side arms.

Acknowledgment. This work was supported by a Grant-in-Aid for Scientific Research (Grants 16550129 and 18550131) from the Ministry of Education, Culture, Sports, Science and Technology (Japan) for Y.H.

Supporting Information Available: X-ray data of **2a**-$AgPF_6$, **2b**-AgOTf, **2c**-AgOTf, **2d**-AgOTf, **2e**-AgOTf, and **2f**-AgOTf (CIF format) and cold ESI-MS data. This material is available free of charge via the Internet at http://pubs.acs.org.

IC700538F

(9) Madhavi, N. N. L.; Katz, A. K.; Carrell, H. L.; Nangia, A.; Desiraju, G. R. *Chem. Commun*. **1997**, 1953. Grossel, M. C.; Cheetham, A. K.; Hope, D. A. O.; Weston, S. C. *J. Org. Chem*. **1993**, *58*, 6654. Takahasi, H.; Tsuboyama, S.; Umezawa, Y.; Honda, K.; Nishio, M. *Tetrahedron* **2000**, *56*, 6185. Evans, D. J.; Junk, P. C.; Smith, M. K. *New J. Chem*. **2002**, *26*, 1043. Guo, W.; Guo, F.; Xu, H.; Yuan, L.; Wang, Z.; Tong, J. *J. Mol. Struct.* **2005**, *733*, 143. Takemura, H.; Iwanaga, T.; Shinmyozu, T. *Tetrahedron Lett.* **2005**, *46*, 6687. Sako, K.; Mase, Y.; Kato, Y.; Iwanaga, T.; Shinmyozu, T.; Takemura, H.; Ito, M.; Sasaki, K.; Tatemitsu, H. *Tetrahedron Lett.* **2006**, *47*, 9151.

(10) Kuppers, H.-J.; Wieghardt, K.; Tsay, Y.-H.; Kruger, C.; Nuber, B.; Weiss, J. *Angew. Chem., Int. Ed. Engl.* **1987**, *26*, 575.

(11) Hehre, W. J. *A Guide to Molecular Mechanics and Quantum Chemical Calculations*; Wavefunction, Inc.: Irvine, CA, 2003; p 72.

(12) Suezawa, H.; Hashimoto, T.; Tsuchinaga, K.; Yoshida, T.; Yuzuki, T.; Sakakibara, K.; Hirota, M.; Nishio, M. *J. Chem. Soc., Perkin Trans.* **2000**, *2*, 1243.